


RESEARCH

Open Access



# Comprehensive biomarker and modeling approach to support dose finding for BI 836880, a VEGF/Ang-2 inhibitor

Sascha Keller<sup>1</sup>, Ulrich Kunz<sup>1</sup>, Ulrike Schmid<sup>1</sup>, Jack Beusmans<sup>2</sup>, Martin Büchert<sup>3</sup>, Min He<sup>4</sup>, Girish Jayadeva<sup>5</sup>, Christophe Le Tourneau<sup>6</sup>, Doreen Luedtke<sup>1</sup>, Heiko G. Niessen<sup>1</sup>, Zohra Oum'hamed<sup>1</sup>, Sina Pleiner<sup>1</sup>, Xiaoning Wang<sup>2</sup> and Ralph Graeser<sup>4,7\*</sup> 

## Abstract

**Background** BI 836880 is a humanized bispecific nanobody<sup>®</sup> that binds to and blocks vascular endothelial growth factor (VEGF) and angiopoietin-2 (Ang-2). A comprehensive biomarker and modeling approach is presented here that supported dose finding for BI 836880.

**Methods** Two Phase I dose-escalation studies (1336.1 [NCT02674152], 1336.6 [NCT02689505]) assessed BI 836880 in adults with confirmed locally advanced or metastatic solid tumors, refractory to standard therapy or for which standard therapy was not reliably effective. Two dosing schedules were investigated, 3 weeks (q3w) or once weekly (qw), starting at a dose of 40 mg. In a comprehensive biomarker approach, soluble pharmacodynamic markers (free and total plasma VEGF-A and Ang-2), as well as circulating angiogenic factors (soluble VEGF3, soluble Tie2 and placenta growth factor, amongst others) were analyzed to assess target engagement in peripheral blood for q3w doses. A Population based pharmacokinetics/pharmacodynamics (PopPK/PD) model was built using the limited Phase I dataset to support dose finding by simulations. In order to demonstrate drug activity in the tumor, dynamic contrast-enhanced magnetic resonance imaging (DCE-MRI) was applied.

**Results** DCE-MRI scans supported target engagement in the tumor. Free VEGF-A was depleted at all doses, whereas free Ang-2 decreased dose-dependently, reaching depletion in most patients from 360 mg q3w onwards. While total VEGF-A levels increased in a dose-dependent manner, reaching saturation at 360 mg q3w, total Ang-2 levels increased, but did not plateau. Angiogenic biomarkers showed changes from doses  $\geq$  360 mg q3w. PopPK/PD modeling showed that doses  $\geq$  360 mg q3w led to  $> 90\%$  inhibition of free Ang-2 at steady-state in most patients. By increasing the dose to  $\geq$  500 mg q3w,  $> 90\%$  of patients are expected to achieve this level.

**Conclusions** The comprehensive analyses of multiple target engagement markers support BI 836880 720 mg q3w as a biologically relevant monotherapy dose schedule.

*Trial registration:* NCT02674152 and NCT02689505.

**Keywords** BI 836880, Biomarkers, VEGF, Ang-2, Pharmacokinetics, Pharmacodynamics

\*Correspondence:

Ralph Graeser

r.graeser17@gmail.com

Full list of author information is available at the end of the article



© The Author(s) 2024. **Open Access** This article is licensed under a Creative Commons Attribution-NonCommercial-NoDerivatives 4.0 International License, which permits any non-commercial use, sharing, distribution and reproduction in any medium or format, as long as you give appropriate credit to the original author(s) and the source, provide a link to the Creative Commons licence, and indicate if you modified the licensed material. You do not have permission under this licence to share adapted material derived from this article or parts of it. The images or other third party material in this article are included in the article's Creative Commons licence, unless indicated otherwise in a credit line to the material. If material is not included in the article's Creative Commons licence and your intended use is not permitted by statutory regulation or exceeds the permitted use, you will need to obtain permission directly from the copyright holder. To view a copy of this licence, visit <http://creativecommons.org/licenses/by-nc-nd/4.0/>.

## Introduction

In 2022, an estimated 20 million cases of cancer were reported and by 2050, this number is expected to increase by approximately 77% [1]. With an overall mortality rate of around 50%, cancer remains a major global health concern [2]. Despite advances in immunotherapy and targeted therapies, chemotherapy remains the standard of care for many types of cancer [3, 4]. However, prolonged exposure to chemotherapy has been associated with excessive toxicities, making the need for effective therapeutic options increasingly critical [3, 4].

Angiogenesis, one of the hallmarks of cancer, is an essential process in tumor growth and metastasis [5, 6], and the vascular endothelial growth factor (VEGF) is one of the key regulators. Binding of VEGF to its receptors on endothelial cells induces angiogenic processes, such as endothelial cell proliferation and migration [7]. VEGF is overexpressed in many cancers and high expression levels are often correlated with poor prognosis [8].

Targeting of VEGF is an established therapeutic strategy in oncology. Bevacizumab—a humanized VEGF-A-specific monoclonal antibody—was first approved for metastatic colorectal cancer in 2004 and is now used in the treatment of several advanced cancers, including metastatic breast cancer, non-small-cell lung cancer, glioblastoma, renal cell carcinoma, ovarian cancer and cervical cancer [9]. Other approaches to targeting the VEGF pathway include the VEGF receptor tyrosine kinase inhibitors (such as sunitinib, sorafenib, nintedanib and lenvatinib) and the VEGF receptor-2 monoclonal antibody, ramucirumab [7]. While these agents have demonstrated substantial clinical benefit in patients with certain advanced cancers, some patients do not respond, and others will eventually experience disease progression because of the development of resistance to treatment. As such, additional research has focused on identifying markers to predict those patients who are most likely to obtain clinical benefit and the role of other angiogenic factors [10].

One pathway of interest is the angiopoietin (Ang)/Tie signaling pathway, which also contributes to blood vessel remodeling: Ang-1/Tie2 signaling stabilizes new blood vessels, while Ang-2/Tie2 signaling destabilizes them [11]. Since stabilizing and destabilizing signals are both transmitted via the same receptor kinase, Tie-2, the destabilizing activity can only be properly addressed via specific Ang-2 blockers.

Given the complementary actions of VEGF and Ang-2 signaling, it is anticipated that combined inhibition may improve antitumor activity. Preclinically, combined VEGF/Ang-2 inhibition showed better antitumor activity than inhibition of either pathway alone [12, 13].

BI 836880 is a humanized bispecific nanobody® comprising two single variable domains that bind to and block VEGF-A and Ang-2, as well as an albumin-binding module for half-life extension in vivo [14]. Preclinically, BI 836880 has been shown to be a potent and selective inhibitor of VEGF-A and Ang-2. BI 836880 showed antitumor activity in a range of patient-derived xenograft models, with superior activity to VEGF-A or Ang-2 inhibition alone [14].

Two Phase I studies were conducted to determine the maximum tolerated dose/recommended Phase II dose of BI 836880 and assess its safety and activity in patients with advanced solid tumors (NCT02674152 and NCT02689505) [15]. Study 1336.1 assessed BI 836880 given intravenously every 3 weeks (q3w) while study 1336.6 assessed BI 836880 given once weekly (qw). BI 836880 demonstrated a manageable safety profile with a maximum tolerated dose of 720 mg q3w (study 1336.1) and 180 mg qw (study 1336.6), respectively. One dose-limiting toxicity (DLT) event occurred at the q3w treatment (grade [G] 3 pulmonary embolism [1000 mg]). Five DLTs occurred in four patients treated qw (G2 proteinuria [120 mg]; G3 hypertension [180 mg]; G3 proteinuria and G3 hypertension [240 mg]; and G4 respiratory distress [240 mg]) [11].

Historically, dose finding for oncology has relied on dose escalation until dose limiting toxicities occurred followed by a dose reduction to determine the maximally tolerated dose. For cytotoxic drugs, like many chemotherapeutics, this was considered a rational approach. However, targeted therapies may show relevant biological effects before toxicity levels have been reached, or may not show dose-limiting toxicities at all. Anti-angiogenic drugs, as was also shown for BI 836880, are generally well tolerated with hypertension as the major on-target toxicity, which can be addressed by co-medication. Determining a biologically active dose is therefore of considerable importance. Also, the FDA has recently started project OPTIMUS to address the issues in defining the right dose in oncology drug development [16–19].

In this report, we describe the analysis of multiple biomarkers in Phase I dose escalation studies to demonstrate BI 836880 target engagement and, in combination with a population based pharmacokinetic/pharmacodynamic (PopPK/PD) modeling approach, support dose decisions for further clinical development. Given the intrinsic difficulty of dose escalation studies with small, heterogeneous patient populations, assays needed to be robust, fit-for-purpose, and validated in order to avoid introducing even more complexity into data analysis. Assay development and validation for the soluble pharmacodynamic (PD) markers of this study

(free and total plasma VEGF and Ang-2) are explained in detail. Results from the measurement of these markers together with a set of complementary angiogenesis-relevant circulating factors (soluble VEGF3 [sVEGFR3], soluble Tie2 [sTie2] and placenta growth factor [PlGF]) are presented, along with the development of the PopPK/PD model. The PK data relevant for the PopPK model development have been published elsewhere [11], and are not topic of the present manuscript. In the absence of tumor measurements of these biomarkers, dynamic contrast-enhanced-magnetic resonance imaging (DCE-MRI) was employed to demonstrate the effect of BI 836880 on the tumor vasculature. The complete dataset was then used to support 720 mg as a biologically active dose.

## Materials and methods

### Patients and study design

Study design and eligibility criteria for studies 1336.1 and 1336.6 have been published previously [15]. In brief, studies 1336.1 and 1336.6 were non-randomized, open-label, dose escalation studies. Adult patients with locally advanced or metastatic solid tumors which were either refractory after standard therapy or for which standard therapy was not reliably effective were enrolled. Patients received BI 836880 via intravenous infusion at a starting dose of 40 mg given q3w or qw. Data from study 1336.1 were used to demonstrate target engagement for different q3w dose levels based on a multiple biomarker approach. In addition, combined data from studies 1336.1 and 1336.6 were considered for population (Pop)PK/PD (Ang-2) modeling. The studies were conducted in accordance with the Declaration of Helsinki and Good Clinical Practice guidelines as defined by the International Conference on Harmonization; all patients provided written informed consent for study participation; and the institutional review board approved the study.

### PK and PD sampling and assays

For quantification of free/total VEGF-A and free/total Ang-2, 6 mL of blood was taken at pre-defined timepoints throughout treatment after the first and repeated doses. In study 1336.1, free/total levels of VEGF-A and Ang-2 were measured on days 1, 2, 3, 8 and 15 in cycles 1, 2 and 4; days 1, 2 and 3 in cycle 3; and day 1 in cycles 5–12. For circulating angiogenic biomarkers, such as sVEGFR3, sTie2 and PlGF, 3 mL of blood was taken at pre-defined timepoints throughout treatment (cycle 2, day 1 for sVEGFR3 and sTie2 and cycle 1, day 3 for PlGF). DCE-MRI scans were performed at baseline, 1 week after administration of BI 836880, after the second treatment cycle (week 6) and after the fourth treatment cycle (week 12) in the absence of progressive disease. DCE-MRI data

acquisition details are provided within the Additional file, including sequence parameters of the MRI protocol (Additional file Table S1). PK samples of BI 836880 were also taken at pre-defined timepoints throughout treatment (days 1, 2, 3, 8 and 15 in cycles 1, 2 and 4; days 1, 2 and 3 in cycle 3; day 1 in cycles 5–12).

### Total VEGF-A

Total VEGF-A levels were determined by a nano liquid chromatography high-resolution mass spectrometry (LC-HRMS) method developed at Boehringer Ingelheim. Recombinant human VEGF165 (Ala27-Arg191) was used as a calibration standard (R&D systems, 293-VE-050, USA). SILuTM Prot VEGF165 (Ala27-Arg191, Merck, MSST0005, Germany) recombinant protein was used as an internal standard, in which all lysine and arginine residues are replaced at a  $\geq 98\%$  rate with heavy labeled analogues (Arg [13C6, 15N4], Lys [13C6, 15N2]). All protein stock solutions and working solutions were prepared and diluted in 0.1% protease-free bovine serum albumin/phosphate buffered saline (PBS) solution. A calibration standard working solution was prepared at a concentration of 10  $\mu\text{gEq/mL}$  and a healthy volunteer K2 ethylenediaminetetraacetic acid (EDTA)-plasma pool was spiked with this working solution at concentration levels of 0, 1, 5, 10, 25 and 50  $\text{ngEq/mL}$ . Each batch included a set of calibration samples and quality control (QC) samples at two different concentration levels (QC.1: 8  $\text{ngEq/mL}$  and QC.2: 40  $\text{ngEq/mL}$  recombinant VEGF-A in healthy K2 EDTA-plasma).

Either 50  $\mu\text{L}$  of study sample or calibration/QC sample was used as input. Internal standard was added to each sample at the beginning of the sample extraction protocol (final internal standard concentration was 5  $\text{ngEq/mL}$ ) to normalize for variable extraction rates of different samples. Samples were diluted with 150  $\mu\text{L}$  50 mM ammonium bicarbonate (ABC) buffer. Afterwards, heat denaturation was performed under rigorous shaking at 95 °C for 5 min to disrupt most biological interactions in the sample. Samples were reduced with 5 mM dithiothreitol at 60 °C for 30 min. The 96-well sample plate was cooled, 15 mM iodoacetamide was added and samples were incubated at room temperature (RT) for 30 min protected from light. Samples were further diluted to a total volume of 8 mL with 5 mM  $\text{CaCl}_2$  in 50 mM ABC buffer. Digestion was performed with 40  $\mu\text{g}$  of bovine pancreas trypsin (Merck, T1426, Germany) at 37 °C overnight. As the achieved digestion rates were insufficient for the required sensitivity of the assay, a further 40  $\mu\text{g}$  trypsin was added and the digestion step at 37 °C was prolonged by 6 h. Any remaining proteolytic activity in the sample was then blocked by the addition of 2.5  $\mu\text{g/mL}$  aprotinin.

For immunoprecipitation, the sample was further diluted by the addition of 400  $\mu\text{L}$  of 10 $\times$ Tris Buffered Saline (TBS-T, Bio-Rad, Germany). Samples were mixed with 20  $\mu\text{L}$  polyclonal anti-VEGF-A antibody (immunogen: “a synthetic peptide derived from N-terminus of human VEGF”, PA5-16754, rabbit, immunoglobulin G, Thermo Fisher Scientific, UK) and incubated under moderate shaking at 4 °C for 3 h. After incubation, 20  $\mu\text{L}$  of a protein A magnetic bead slurry (Thermo Fisher Scientific, 10001D, Germany) was added and samples were incubated on a rolling wheel at 4 °C overnight. Washing steps were performed on a King Fisher Flex magnetic bead handling system (Thermo Fisher Scientific, UK) using the following washing solutions: wash 1: 300  $\mu\text{L}$  of 0.5 $\times$ TBS-T, wash 2: 200  $\mu\text{L}$  of 0.5 $\times$ TBS-T, wash 3 and 4: 200  $\mu\text{L}$  of 10 mM HEPES/KOH, pH 7.9. Peptides were eluted from the beads with 150  $\mu\text{L}$  0.25% trifluoroacetic acid (TFA). Supernatants were transferred and further purified by SOLA $\mu$  HRP 2 mg/mL 96-well solid phase extraction plates (Thermo Fisher Scientific, Germany) according to manufacturer’s instructions by using a positive pressure manifold (Waters, USA). Finally, peptides were eluted twice from the solid phase extraction plate by 35  $\mu\text{L}$  of 70% acetonitrile (ACN). Organic solvents were removed by evaporation at 40 °C and samples were reconstituted in 30  $\mu\text{L}$  sample buffer (0.1% TFA, 0.5% acetic acid, 2% ACN in water).

10  $\mu\text{L}$  of the sample was injected into an NCS-3500RS nano LC system (Thermo Fisher Scientific, USA). A standard 70 min gradient was run (buffer A: 0.5% acetic acid in water; buffer B: 0.5% acetic acid in ACN; gradient 0–7 min: 5% buffer B; 30 min: 14.5% buffer B; 40 min: 45% buffer B; 45–55 min: 85% buffer B; 59–70 min: 5% buffer B) at a flow rate of 300 nL/min. An Acclaim PepMap 100 trap column (100  $\mu\text{m}\times 2\text{ cm}$ , C18, 5  $\mu\text{m}$ , 100 Å, Thermo Fisher Scientific, Germany; loading buffer: 0.1% TFA, 1% ACN in water) was used to pre-focus the peptides. Peptides were separated on an Easy-Spray column (75  $\mu\text{m}\times 15\text{ cm}$ , C18, 3  $\mu\text{m}$ , 100 Å, Thermo Fisher Scientific, Germany) heated to 40 °C. “APM[MetO]<sup>s</sup>AEGGGQNHHEVVK” 3+ and 4+ precursor ion currents (elution time: 15.6 min; mass [3+]: 559.5984, mass [4+]: 419.5907) and “APM[MetO]AEGGGQNHHEVVK [1 $\times$ deamidation, (N,Q)]” 3+ and 4+ precursor ion currents (elution time: 15.6 min; mass [3+]: 559.9265, mass [4+]: 420.1967), as well as their corresponding heavy analogues, were recorded on a Q Exactive high field high resolution mass spectrometer (Thermo Fisher Scientific, USA) operated in the full scan-ddMS2 modus (mass accuracy < 5 ppm). The resolution for full scan experiments was set to 60,000 (at  $m/z$  200) and automatic gain control target to 1e6 ions (range:

350–1600  $m/z$ ). For ddMS2-experiments, the resolution was set to 30,000 and automatic gains control target to 1e5 ions. 3+ and 4+ precursor peak areas were summed up to gain more intensity. Summed “APM[MetO]AEGGGQNHHEVVK” signals were used as quantifier, while summed “APM[MetO]AEGGGQNHHEVVK [1 $\times$ deamidation, (N,Q)]” signals were used as qualifier. Neither unmodified peptide forms nor other prominent modifications, other than the two described, were detected (in validation nor in study samples). As the calibrator used in this study was not fully characterized, the assay was considered as relative quantitative.

#### Free VEGF-A

Free VEGF-A was measured using a commercial electrochemiluminescence immunoassay kit without major modification (Human VEGF V-Plex Kit, Cytokine Panel 1, Meso Scale Discovery, USA, K151RHD). The sandwich assay uses monoclonal anti-VEGF-A antibodies as capture and detection reagents. One of them competes with the anti-VEGF-A binding epitope of BI 836880. It was calibrated relative to the recombinant standard from the kit. Plasma samples were measured without further preparation in a fixed dilution of 1:2. The assay was performed in a semi-automated manner using a Hamilton Star liquid handling system for dilution of samples and distribution to the microtiter plate as well as a microtiter plate robot for automated performance of all incubation, washing, addition of reagents and reading of response steps of the immunoassay. This system has been developed at Boehringer Ingelheim.

#### Total Ang-2

Total Ang-2 was analyzed using a modified and automated commercial enzyme-linked immunosorbent assay (ELISA) kit from BioTechne (R&D Systems, USA #SANG20). The standard sandwich ELISA uses a monoclonal anti-Ang-2 capture antibody immobilized to the microtiter plate and a second monoclonal anti-Ang-2 detection antibody. As reference standard, bulk material of one lot was banked in aliquots at – 70 °C (623-AN-025, R&D Systems/BioTechne Inc. USA). The assay was calibrated relative to this recombinant standard material. The lyophilized standard was reconstituted, diluted in assay buffer and stored as single-use working aliquots at – 70 °C. The stability of the ready-to-use calibration samples has been proven for several years. Simple thawing of the calibration samples reduces the workload on each measuring day and also the assay variability. The assay was performed according to the kit manual with one modification. After washing of the uncovered microtiter plate, 90  $\mu\text{L}$  of assay diluent that had been spiked with 100 ng/mL drug was dispensed in each well of

the plate. Thereafter 50  $\mu$ L of the diluted plasma samples, quality controls and calibrators were added in duplicates (one sample in two wells). After 4 h of incubation at RT on a shaker the plate was washed, the detection antibody conjugated to horseradish peroxidase was added, and the plate was incubated for another 2 h at RT. Final steps were washing, addition of tetramethylbenzidine substrate solution, incubation in the dark for 30 min, addition of stop solution (1 M phosphoric acid) and reading of responses (difference responses at 450–650 nm). The Ang-2 concentration corresponding to the measured optical absorbance was calculated via data fitting of the non-linear 4-parameter logistic standard curve obtained by measuring the calibration samples prepared from the recombinant human Ang-2. Distribution of samples to the microtiter plate was performed on a Hamilton Star liquid handling system in a randomized manner. The steps of the ELISA process were automated on a robotic system developed at Boehringer Ingelheim.

#### **Free Ang-2**

Free Ang-2 was analyzed using an ELISA developed at Boehringer Ingelheim. The sandwich assay uses the biotinylated anti-Ang-2 therapeutic nanobody as capture reagent immobilized to the streptavidin coated microtiter plate (StreptaWell High Bind Plates, Roche Diagnostics GmbH, Germany). It captures all “free” Ang-2 from the plasma sample that has not been blocked by the drug. After washing of the plate, 25  $\mu$ L of assay buffer was added to each well to prevent drying of the plate. Then 100  $\mu$ L of calibrators, quality controls and plasma samples were added. The calibrators were prepared from the same reference standard as in the total Ang-2 ELISA and diluted in PBS+0.1% Casein Blocker (Bio-Rad, USA)+0.05% Tween 20. All plasma samples were diluted in the minimum required dilution of 1:2 in the same assay buffer. After incubation for 4 h at RT on a shaker, the plate was washed and the mouse monoclonal anti-Ang-2 detector antibody was added (R&D Systems Inc., USA, MAB0983). Two hours later, the immune complexes formed on the plate surface were detected by a goat anti-mouse secondary antibody labeled with horseradish peroxidase (#31439, Thermo Fisher, USA) for 1 h at RT. The plates were then washed and 100  $\mu$ L per well tetramethylbenzidine Super Sensitive Microwell One Component Peroxidase substrate (BioFX Laboratories, L.L.C., USA) was added. After incubating in the dark for 30 min, 100  $\mu$ L 1 M phosphoric acid was added to terminate the enzyme reaction and the adsorption was read at 450–650 nm. The Ang-2 concentration corresponding to the measured optical absorbance was calculated via data fitting of the non-linear 4-parameter logistic standard

curve. The same automated equipment was used as for the total Ang-2 ELISA.

#### **Circulating angiogenic factors**

Circulating angiogenic factors such as sTie2, sVEGFR3 and PlGF were analyzed in K2 EDTA plasma using a multi-analyte profiling (MAP) immunoassay kit (Angiogenesis MAP®; Rules-Based Medicine [RBM]).

#### **DCE-MRI**

DCE-MRI scans were conducted to provide non-invasive quantification of microvascular structure and function properties, such as vascular permeability, vascular density and regional vascular flow, within tumor lesions. DCE-MRI data acquisition details are provided within the Additional file (Table S1).

#### **BI 836880 plasma concentrations**

BI 836880 plasma concentrations were quantified using a validated bioanalytical assay [11].

#### **Data analysis**

##### **Biomarker and imaging data analysis (study 1336.1)**

Mean time profiles of free and total VEGF-A and Ang-2 in study 1336.1 were summarized by treatment group using exploratory plots. Likewise, levels of sVEGFR3, sTie2 and PlGF at baseline and following treatment with BI 836880 q3w were explored graphically by treatment group.

For DCE-MRI analysis, only patients with lesions considered suitable for DCE-MRI by a radiologist (preferably liver metastases >2 cm) were included to minimize methodological variability. All patients who had at least two DCE-MRI measurements were included in the analysis. DCE-MRI images were analyzed using dedicated software, *MRDAC perfusion tool V5*.

Initial area under the contrast agent concentration–time curve at 60 s (iAUC60) and the transfer constant (Ktrans) were reported for each imaging time point. iAUC60 is a model free parameter while Ktrans results from quantitative modeling [20] of tissue gadolinium concentration–time curve using a multi-compartmental model. Time profiles of Ktrans and iAUC60 and their changes from baseline were summarized using descriptive statistics.

##### **PopPK/PD (Ang-2) modeling (studies 1336.1 and 1336.6)**

PopPK/PD modeling of BI 836880 in patients with solid tumors was performed based on combined measurements of total BI 836880 and free and total Ang-2 in plasma from studies 1336.1 and 1336.6. Free and total VEGF-A were not included as PD endpoints

because free VEGF-A levels were below the lower limit of quantification (LLOQ) at all sampling times and all dose levels (indicating full blockage) and total VEGF-A levels were measured in only a limited number of patients. A sequential modeling approach was applied first establishing a PopPK model for BI 836880. A PD model was then developed using individuals' plasma concentrations of BI 836880 predicted from the PK model. Interindividual variability (IIV) and interoccasion variability (IOV) were modeled using exponential random effect models and a full covariance matrix. IIV, IOV and residual (unexplained) variability were assumed to be symmetrically distributed around 0. IIV was included on all PK or PD model parameters wherever possible. IOV was included on Ang-2 synthesis to accommodate for the variability in total Ang-2 levels over time. An initial covariate screening of PK parameters was performed considering the covariates of gender, body weight, human serum albumin (HSA), estimated glomerular filtration rate (eGFR), alkaline phosphatase (ALP), Eastern Cooperative Oncology Group (ECOG) performance status, anti-drug antibodies, country of study site location and study. HSA, eGFR and ALP were included as time-varying covariates, whereas the other covariates were implemented as time-independent covariates (baseline covariates). No covariate was missing in more than 10% of the patients. The missing covariates were imputed with the median of the remaining values (for baseline covariates) or by last observation carried forward imputation (for time-varying covariates). Model selection was guided by change in objective function values, identifiability of parameters and precision of parameter estimates, correlation between the estimates of fixed effect parameters, numerical stability, ability to obtain a successful COVARIANCE step and visual inspection of basic goodness-of-fit plots. The covariate-parameter relationships were first evaluated using exploratory graphics (including graphical inspection of IIV versus baseline covariates plots) combined with an assessment of scientific interest and prior knowledge of mechanistic plausibility. Afterwards, a full covariate model was constructed with covariate-parameter relationships selected in the first step taking care to avoid correlation or collinearity in predictors (covariates with correlation coefficients  $>0.35$  were not simultaneously included as potential predictors). Inferences about relevance of covariate effects were based on the resulting parameter estimates of the full model and measures of estimation precision (asymptotic standard errors, bootstrap 95% confidence intervals [CI] or log-likelihood

profile). No hypothesis testing was conducted. Under circumstances that some covariate effects were estimated with large uncertainty, the full PK model was simplified to a final PK model by removing these covariate effects. No covariates were included in the PD model. A sensitivity analysis was conducted comparing different approaches of handling the large percentage of measurements below the limit of quantification (BLQ) for free Ang-2 samples. Besides discarding BLQ values from model development, methods were explored, in which the probability of a sample being BLQ is calculated and included as part of the model's objective function (M3 method) [18]. In addition, the assignment of a value of less than the LLOQ ( $\text{LLOQ} \times 0.99$ ,  $\text{LLOQ}/2$ ,  $\text{LLOQ}/3$ ) to all BLQ values or by merging all consecutive BLQ values to one value was evaluated. All analyses were conducted via nonlinear mixed-effects modeling with a qualified installation of the nonlinear mixed effects modeling software NONMEM, Version 7.3 (ICON Development Solutions, Hanover, MD, USA). The final model was evaluated by visual predictive checks (VPCs) assessing the model's ability to reproduce overall trends and variability in the observed data. Therefore, 500 Monte Carlo simulation replicates of studies 1336.1 and 1336.6 were generated using the developed population PK/PD model. For the VPC, plots of the observed data were constructed and overlaid with the simulated median and 10th and 90th percentiles.

The PopPK/PD model was used to simulate PK and PD profiles of BI 836880 and to summarize the probability of achieving minimal inhibition levels of free Ang-2 of 90% and 95% at trough concentrations of BI 836880 (defined as target attainment). The simulation population consisted of 1000 patients whose baseline covariate values were obtained by randomly and jointly sampling from appropriate multivariate parametric approximations of the covariates' observed values in both studies 1336.1 and 1336.6. Individual PK parameters were obtained from the PopPK model. The sources of variability included IIV and IOV in the PK and the PD model, as well as parameter uncertainties in both models.

Simulated treatment consisted of 3-week treatment cycles (q3w dosing), with each treatment cycle consisting of a single infusion with a nominal infusion duration of 90 min at the start of the cycle. Simulated dose levels of BI 836880 per infusion were 40, 120, 360, 500 or 720 mg. The probability of target attainment (median and 5th and 95th percentiles) was calculated as a function of treatment cycle and dose. The simulation was repeated 1000 times to calculate CIs for the predicted probabilities of target attainment.

## Results

### Free and total VEGF-A and Ang-2 assay development and validation

#### Context of use

The direct targets of BI 836880, Ang-2 and VEGF-A, were quantified in EDTA plasma from patients as markers of target engagement to prove the pharmaceutical principle and support dose selection by means of the PopPK/PD model.

Modelling of the drug–target equilibria requires the separate, specific determination of the free and the total soluble target concentrations (see glossary box for definitions). It was expected that total target levels would increase after multiple treatments due to prolongation of target half-life, whereas free target levels were expected to decrease due to drug–target complex formation. The assays were required to be specific for total and free target, precise, parallel (see glossary box for definitions) and sensitive enough to detect a 90% decrease from baseline of healthy volunteer levels (free Ang-2, free VEGF-A). For total Ang-2 and total VEGF-A, a sensitivity in the range of healthy volunteer baseline levels was considered sufficient. All assays needed to be robust enough to guarantee comparability of results during clinical development of the drug. This would include an assay monitoring program based on banked sample controls, reference standards and careful bridging of lot changes of the calibration standard and critical reagents [21].

EDTA plasma was chosen as sample matrix for all assays as VEGF-A levels in serum are artificially increased by its release from platelets during coagulation, leading to a distortion of the original endogenous level in plasma [22]. Assay development is described in detail in the Supplementary Material.

#### Analytical performance (validation)

A series of validation experiments were performed to confirm the suitability of the four assays (Table 1). Further experiments considered stability of whole blood samples, influence of centrifugation speed, stability of stock solution, calibration samples and coated plates; and robustness of assay when performed by different scientists (data not shown). Assay validation was successful for all four assays confirming their suitability for use in the Phase I clinical study.

#### Patient sample measurement

Assay performance during sample measurement from the clinical Phase I studies was comparable to the performance during validation. Between-run precision of the QC samples was in the expected range for each of the assays.

To compare the free and total Ang-2 assays, 53 pre-dose EDTA plasma samples from patients were analyzed with both ELISAs. The results were correlated using the Excel Ad-in Analyze-it and the Spearman correlation function. Correlation was high ( $\rho=0.9$ ) and the linear regression showed a slope of 1.14 between free and total Ang-2 results (Additional file Fig S1C). The free Ang-2 ELISA quantifies about a 14% higher level in the baseline samples without drug than the total Ang-2 ELISA which is mainly caused by the bias in the total Ang-2 ELISA due to addition of drug to each sample.

### Biomarker and imaging data analysis (study 1336.1)

#### Free/total VEGF-A and free/total Ang-2 levels during BI 836880 treatment

Pre-dose VEGF-A levels ranged from 0.022 to 0.669  $\mu\text{gEq/L}$ . Systemic free VEGF-A was completely blocked (below LLOQ) for all doses (Fig. 1A). Free VEGF-A remained blocked until the next treatment cycle. A dose-dependent increase of total VEGF-A levels was observed. Total VEGF-A levels appeared to reach saturation at  $\geq 360$  mg q3w (Fig. 1B). Pre-dose free Ang-2 levels ranged from 0.72 to 13  $\mu\text{gEq/L}$ . Free Ang-2 was dose-dependently blocked, reaching depletion in most patients at doses of  $\geq 360$  mg q3w, and remained blocked until the next treatment cycle, again in most patients (Fig. 1C). Total Ang-2 levels increased after BI 836880 treatment but did not appear to plateau (Fig. 1D).

#### Other angiogenic marker levels during BI 836880 treatment

Additional angiogenesis-related proteins were analyzed using the RBM Angiogenesis MAP panel. This panel contains, amongst others, angiogenesis-related factors that may to some degree complement the loss of Ang-2 and VEGF-A, as well as soluble receptors, which are known to regulate the levels of their ligands in the blood.

sVEGFR3 and sTie2 levels decreased compared with baseline at BI 836880 doses of  $\geq 360$  mg q3w (Fig. 2A and B). PlGF levels increased versus baseline at doses of  $\geq 360$  mg q3w (Fig. 2C). No similarly consistent changes were observed in any of the other analytes (data not shown).

#### DCE-MRI analysis

DCE-MRI has been used successfully to measure changes in tumor vessel permeability, an important measure of anti-angiogenic drug activity. The volume transfer constant Ktrans assesses capillary permeability using a PK model describing the volume transfer coefficient of the gadolinium-based contrast agent between the blood plasma and the extracellular extravascular leakage space [19].

**Table 1** Summary of key validation parameters of the three immunoassays and LC-HRMS method

Validation parameter	Total Ang-2 ELISA	Free Ang-2 ELISA	Free VEGF-A MSD assay	Total VEGF-A LC-HRMS
Calibration range	0.05–2 ngEq/mL	0.04–1.5 ngEq/mL	3.7–1000 pgEq/mL	1–50 ngEq/mL
LLOQ (at minimum required dilution)	0.1 ngEq/mL (1:2), S/N ( $C_{low}$ /blank) = 1.4	0.08 ngEq/mL (1:2), S/N ( $C_{low}$ /blank) = 1.3	7.4 pgEq/mL (1:2), S/N ( $C_{low}$ /blank) = 3	1 ngEq/mL, S/N (LLOQ/blank) = 5
Intra-assay precision	2% (LLOQ 4%) CV, n = 7 runs × 3 aliquots	2–5% (LLOQ 8%) CV, n = 7 runs × 3 aliquots	3–5% CV (n = 5 runs × 3)	4% CV (QC.1, quantifier), 2% CV (QC.2, quantifier), n = 2 runs × 7 aliquots
Inter-assay precision	3% (LLOQ 6%) CV, n = 3 aliquots × 7 runs	4–11% (LLOQ 24%) CV, n = 3 aliquots × 7 runs	5–8% CV (n = 3 aliquots × 6 runs)	8% CV (QC.1, quantifier), 7% CV (QC.2 quantifier), n = 2 runs × 7 aliquots and n = 2 runs × 3 aliquots
Basal levels healthy volunteers EDTA plasma = biological inter-subject variance	1–5 ngEq/mL, median: 1.8 ngEq/mL, CV 42% (n = 24 subjects)	0.7–6 ngEq/mL, median: 1.7 ngEq/mL, CV 57% (n = 22 subjects)	12–74 pgEq/mL, mean 29 pgEq/mL, CV 50% (n = 20 subjects)	Not detectable
Biological longitudinal intra-subject variance	7% CV (n = 3 healthy volunteers × 15 samples within 1 week), no circadian rhythm	8% CV (n = 3 healthy volunteers × 15 samples within 1 week), no circadian rhythm	36% CV (n = 3 healthy volunteers × 15 samples within 1 week), no significant circadian rhythm	N/A
Short term stability endogenous analyte	+ 3 F/T cycles (– 20 °C, – 70 °C), > 24 h RT	+ 3 F/T cycles (– 20 °C, – 70 °C), > 19 h RT	+ 3 F/T cycles (– 20 °C, – 70 °C), > 4 h RT, slight instability at – 20 °C	+ 2 F/T cycles (– 70 °C), > 4 h RT
Long term stability endogenous analyte (isochronic approach)	> 36 months at – 20 °C and – 70 °C	> 36 months at – 20 °C and – 70 °C	> 36 months at – 20 °C and – 70 °C	N/A
Parallelism	Yes (1:2–1:20,000, n = 6)	Yes (1:2–1:50, n = 6)	Yes (1:2–1:20, n = 4)	Not needed due to undetectable VEGF-A levels in the plasma of healthy volunteers
Selectivity (lipemic, hemolytic plasma)	No interference	No interference	No interference of lipemic plasma but significant interference of hemolytic plasma > 0.5 vol% hemolytic blood	No interference (only performed in sample buffer)
Specificity (second target, drug)	No interference of 100 ng/mL of VEGF-A; no interference of drug up to 100 µg/mL	No interference of 100 ng/mL of VEGF-A; strong interference of drug as expected	No interference of 10 ng/mL of Ang-2; strong interference of drug as expected	N/A
Autosampler stability (8 °C)	N/A	N/A	N/A	20 days (dev. QC.1: 1.2%, dev. QC.2: 9%)

Ang-2, angiotensin-2;  $C_{low}$ , low concentration; CV, coefficient of variation; dev, deviation; EDTA, ethylenediaminetetraacetic acid; ELISA, enzyme-linked immunosorbent assay; F/T, freeze/thaw; LC-HRMS, liquid chromatography/high-resolution mass spectrometry; LLOQ, lower limit of quantification; MSD, Meso Scale Discovery; N/A, not applicable; ngEq, nanogram equivalent; QC, quality control; RT, room temperature; S/N, signal to noise ratio; VEGF-A, vascular endothelial growth factor

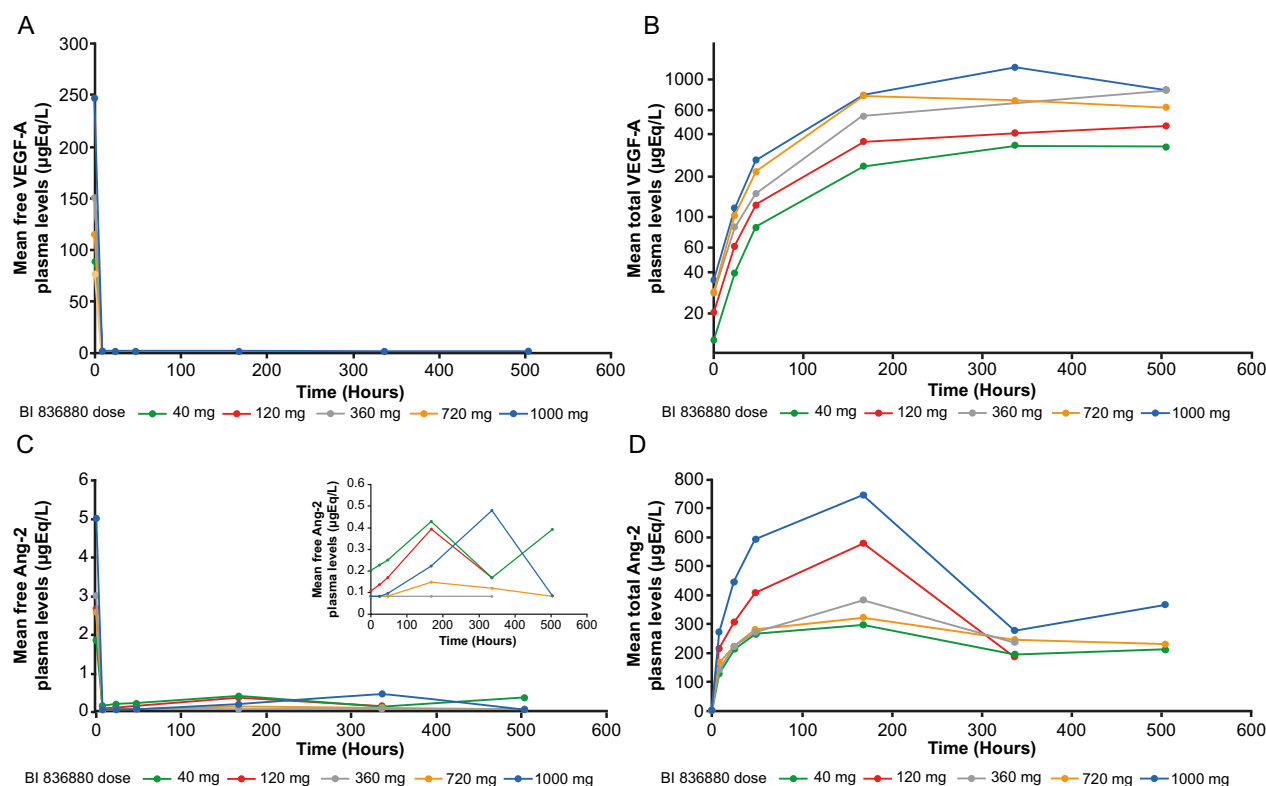


**Fig. 1** Mean free VEGF-A (A), total VEGF-A (B), free Ang-2 (C), total Ang-2 (D) plasma levels over time in patients treated with increasing doses of BI 836880. For A, C, D, the number of patients per dose level at baseline were as follows: 40 mg,  $n=3$ ; 120 mg,  $n=2$ ; 360 mg,  $n=2$ ; 720 mg,  $n=17$ ; 1000 mg,  $n=5$ . However, on-treatment numbers may decrease as patients dropped out of the study. **B** Due to the complexity of the assay, only 2 patients per dose level were analyzed. **C** The inset shows the same data on a different scale in order to improve readability. Standard deviations are not included, since for some dose levels and graphs only 2 patients have been included, and numbers of observations may vary between timepoints even at the same dose level. Ang-2: angiotensin-2; VEGF-A: vascular endothelial growth factor

DCE-MRI analysis was conducted in 14 patients in study 1336.1 (120 mg q3w,  $n=1$ ; 720 mg q3w,  $n=12$ ; and 1000 mg q3w,  $n=1$ ). Clinically meaningful ( $\geq 40\%$ ) reductions in  $K_{\text{trans}}$  [19] were observed in 9 patients (7 patients in the 720 mg group and one each from the 120 mg and 1000 mg groups; Fig. 3A). DCE-MRI scans from a patient whose tumor vessel permeability, as determined via  $K_{\text{trans}}$ , was reduced by 80% compared to baseline after 2 weeks of treatment are presented in Fig. 3B.

#### PopPK/PD modeling (studies 1336.1 and 1336.6)

A two-compartment PK model well described the measured plasma concentrations of BI 836880 from studies 1336.1 and 1336.6 both at the population (Additional file Fig S3) and individual levels and PK was approximately dose linear. Based on a graphical inspection of predefined covariate-parameter relationships for PK, body weight at baseline was included as a covariate on volumes and clearance PK parameters in the full PopPK covariate model (see glossary box for explanations of some of the modelling-related terms). As the precision of the body

weight exponents was low, with 95% CIs approaching the value of 0, a fixed body weight exponent of 0.75 was used for clearance parameters and an exponent of 1 was used for volume parameters. Additional covariates implemented in the full covariate model consisted of HSA, ALP, eGFR, gender and ECOG performance status for the parameter of systemic clearance. Both exploratory plots of covariate parameter relationships and model-based parameter estimation showed that BI 836880 clearance increased with increasing body weight and with decreasing HSA. As such, these covariates were kept in the final model. The covariates of ALP, eGFR and ECOG performance status were associated with small effect sizes on PK and resulted in high uncertainty in parameter estimation. Therefore, these covariates were removed from the final PopPK model. In summary, the inclusion of covariate effects only explained to a minor extent PK variability in the population. Of the five covariates included on clearance (CL) in the full covariate model (Sex, eGFR, ALP, HSA, and ECOG) only HSA had a statistically significant, but minor effect on CL, considering the narrow

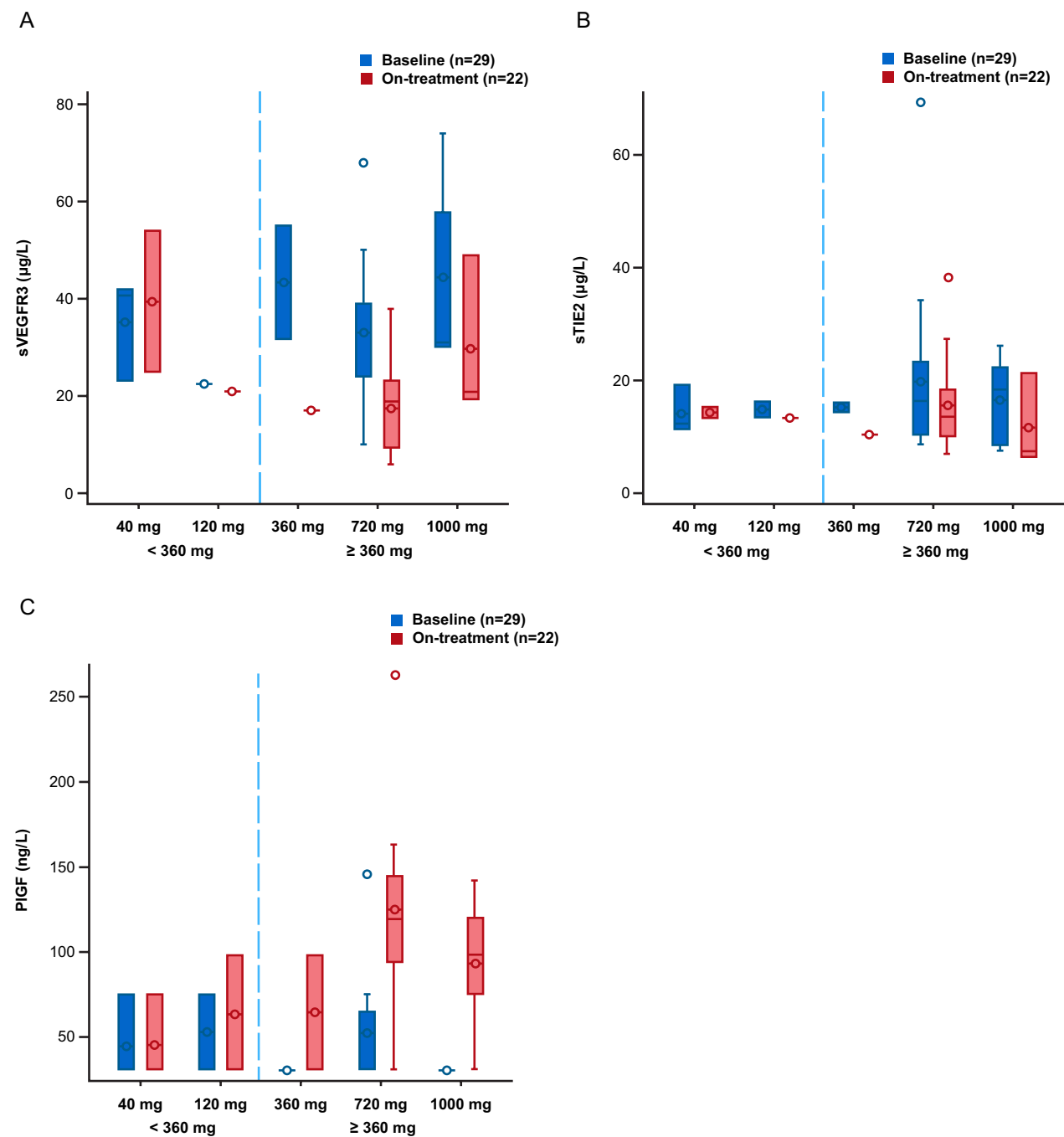


**Fig. 2** Levels of sVEGFR3 (A), sTie2 (B) and PlGF (C) at baseline and On-treatment (cycle 2, day 1 for sVEGFR3 and sTie2 and at cycle 1, day 3 for PlGF), per dose level. The number of patients per dose level are indicated above each boxplot. PlGF: placenta growth factor; sTie2: soluble Tie2; sVEGFR3: soluble vascular endothelial growth factor receptor 3

range of HSA in the patient population (Additional file Table S2).

Using PopPK model estimated PK parameters, the PD model was developed as a mass action model in which BI 836880 in the central compartment binds free Ang-2 and sequesters it in a complex, which degrades with a rate estimated by the model; the model also estimated the rate of synthesis of Ang-2. In addition to the included covariate effects on PK as described above, the sources of variability included IIV and IOV in PK

and PD parameters as well as additive and proportional residual variability terms for the different PK and PD measurements. In order to increase model stability, shared IIVs for parameters with high correlations in IIV were assumed (as outlined in Additional file Table S2). PK and PD model parameter estimates of the final PopPK/PD model are shown in Additional file Table S2 and Table S3, respectively.

Goodness-of-fit evaluations and VPCs demonstrated consistency of final model predictions with observed data with no systematic bias except for an underprediction of the probability of free Ang-2 being BLQ observed in the higher dose groups for study 1336.6 (with weekly treatment schedule). This potential bias was not observed for study 1336.1 including the relevant 3-week treatment schedule (q3w dosing; Additional file Fig S4 and Fig S5).

During sensitivity analyses exploring the handling of high number of BLQ values for free Ang-2 samples, it was not possible to use the method referred to as M3 [23] due to model instabilities. In contrast to this, merging all consecutive BLQ values to one value (assigned to LLOQ/2) gave reasonable results in terms of fitting the free Ang-2 data of individual patients and reproducing the observed patterns of samples that were BLQ. This implementation was therefore kept in the final PopPK/PD model.

PopPK/PD model-based simulations were performed to compare the degree and duration of Ang-2 inhibition for various dose levels considering IIV in the analyzed population of studies 1336.1 and 1336.6 as well as parameter uncertainty as implemented in the final PopPK/PD model. A high degree of Ang-2 inhibition at BI 836880 dose levels of 360, 500 and 720 mg q3w was predicted with most patients reaching >90% free Ang-2 inhibition over the complete treatment cycle at steady-state. For dose levels of 500 mg and 720 mg q3w, more than 90% of patients were predicted to have >90% inhibition of Ang-2 over the complete treatment cycle at steady state (91.4% and 95.6% of patients, respectively; Table 2; Additional file Fig S6).

## Discussion

In this paper, we present a multiple biomarker approach to support dose selection of BI 836880, a VEGF/Ang-2 inhibitor, in a Phase I dose escalation study. The simultaneous analysis of various biomarkers allowed a comprehensive assessment of target engagement and activity for BI 836880 and supported dose selection at a time where limited clinical activity data were available.

Assays to measure free and total Ang-2 and VEGF-A were specifically developed and validated for this study. The requirement for antibody pairs that bind to the target independently, and do not interfere with drug binding, made the development of total target assays challenging. Interference of drug in the commercial Ang-2 ELISA could be saturated and therefore compensated to allow use of the ELISA as a total Ang-2 assay for post-dose samples containing BI 836880. In contrast, the only approach to quantify total VEGF-A was use of a LC-HRMS assay. This approach was used due to interference of the drug in all tested antibody combinations for the total VEGF-A immunoassay which could not be compensated by saturation of the samples with drug.

Our analyses demonstrated that free VEGF-A, but not free Ang-2, levels were depleted at all dose levels of BI 836880 from 40 to 720 mg. Depletion of free Ang-2 was dose-dependent and observed from 360 mg q3w onwards in most patients. The overall reduction of free VEGF-A and Ang-2 levels served as a proof of the mechanism of action of BI 836880. Vanucizumab, a bispecific monoclonal antibody targeting VEGF and Ang-2, also showed reductions in free VEGF-A and Ang-2 [24]. Similarly, bevacizumab has been shown to reduce free VEGF [25, 26].

Total Ang-2 and VEGF-A levels increased dose-dependently upon treatment with BI 836880, likely due to a prolonged half-life of the targets when bound to BI 836880 (due to its HSA-binding, the half-life of BI 836880 is around 11 days). Similar increases were observed during treatment with vanucizumab [24]. An increase of VEGF-A and Ang-2 synthesis may also contribute, however, there is no direct evidence to support this hypothesis. Whereas total VEGF-A levels appeared

(See figure on next page.)

**Fig. 3** Change of tumor blood flow and/or permeability as determined by DCE-MRI in patients treated with BI 836880 in study 1336.1. Ktrans was determined via a model that describes the volume transfer coefficient of the gadolinium-based contrast agent between the blood plasma and the extracellular extravascular leakage space. **A** The percent change of Ktrans from baseline to week 2, 6, and/or 12 after treatment onset. **B** An example of a DCE-MRI scan from baseline (left) and the first follow up scan 2 weeks after treatment with BI 836880 (right) from a patient of the 1000 mg cohort with a not otherwise defined neoplasm, for whom an 80% reduction in Ktrans was calculated. Ca: carcinoma; DCE-MRI: dynamic contrast-enhanced-magnetic resonance imaging; ER+: estrogen receptor positive; Her2: human epidermal growth factor receptor 2 negative; Ktrans: transfer constants

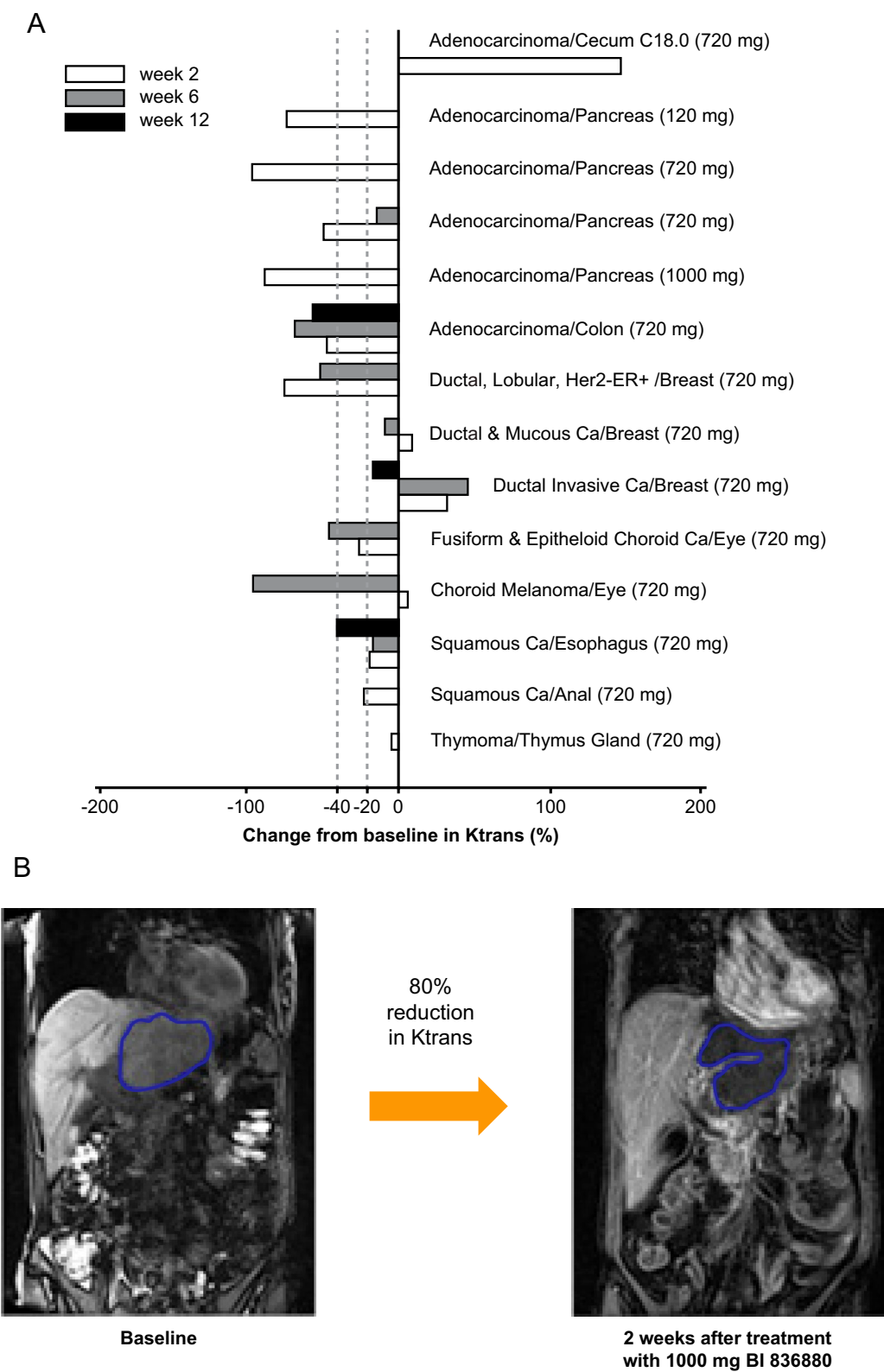


**Fig. 3** (See legend on previous page.)

**Table 2** Ang-2 inhibition at the end of each 3-week treatment cycle

BI 836880 dose	Cycle	Percentage patients	
		> 90% Ang-2 inhibition	> 95% Ang-2 inhibition
40 mg	1	8.8 (4.8–13.7)	1.8 (0.6–3.7)
	2	14.2 (8.7–20.6)	3.5 (1.4–6.7)
	3	16.5 (10.6–23.7)	4.4 (1.9–8.1)
	4	17.4 (11.0–24.6)	4.8 (2.2–8.7)
	5	17.7 (11.5–25.0)	5.0 (2.4–8.7)
120 mg	1	35.3 (26.2–44.2)	13.8 (8.1–19.8)
	2	46.9 (36.4–55.7)	21.4 (13.9–29.5)
	3	50.4 (40.1–59.9)	24.3 (16.5–32.9)
	4	51.8 (41.3–61.1)	25.6 (17.6–34.1)
	5	52.1 (41.9–61.4)	26.0 (17.7–34.7)
360 mg	1	73.8 (64.8–81.2)	47.5 (37.0–57.1)
	2	82.5 (75.1–88.6)	59.6 (49.1–68.4)
	3	84.4 (77.4–90.4)	62.9 (52.4–72.1)
	4	85.4 (77.9–90.8)	64.4 (53.9–73.2)
	5	85.5 (78.6–90.7)	64.6 (54.5–73.6)
500 mg	1	82.8 (75.3–88.7)	59.7 (49.8–69.1)
	2	89.2 (83.5–93.7)	71.0 (61.4–79.0)
	3	90.6 (84.8–94.8)	73.7 (64.5–81.7)
	4	91.2 (85.7–94.9)	75.0 (65.6–82.5)
	5	91.4 (86.0–95.2)	75.2 (66.5–82.6)
720 mg	1	90.1 (84.4–94.4)	72.4 (62.9–80.3)
	2	94.3 (90.0–97.0)	81.5 (73.8–87.9)
	3	95.2 (91.3–97.7)	83.6 (76.1–89.8)
	4	95.4 (91.8–97.9)	84.5 (76.7–90.4)
	5	95.6 (91.6–98.0)	84.7 (77.4–90.3)

Inhibition of Ang-2 based on PopPK/PD model simulations. Numbers present medians (95% confidence interval) based on 1000 simulations of 1000 patients each, considering interindividual variability and parameter uncertainty  
 Ang-2: angiopoietin-2; PopPK/PD: population pharmacokinetics/pharmacodynamics

to reach saturation at 360 mg q3w or higher, total Ang-2 levels did not reach an obvious plateau and the dose dependency was partly non-monotonic. This observation cannot be clearly explained based on the limited number of patients per dose group. However, in the dose groups of 120 mg and 1000 mg, where particularly high levels of total Ang-2 were observed, some patients showed still detectable, albeit very low, levels of free Ang-2 while on treatment (2 and 5 patients at 120 mg and 1000 mg, respectively). This suggests that some patients may be capable of increasing Ang-2 to higher levels than others (e.g. due to IIV in the turnover rate of Ang-2), providing a potential explanation for the higher total levels found in the 120 mg and 1000 mg groups as compared to the other dose groups.

As part of the RBM Angiogenesis MAP, levels of soluble receptors, which may serve as ligand traps to regulate Ang-2 and VEGF levels, were analyzed. The amount of sVEGFR3 (receptor of VEGF-C and VEGF-D) decreased during BI 836880 treatment. A decrease of sTie2, the soluble Ang-2 receptor, was also observed. We also analyzed levels of other ligands that can contribute to angiogenesis and showed that levels of PlGF (an alternative ligand to VEGFR1) increased during BI 836880 treatment. This might reflect the body's attempt to counteract the systemic loss of VEGF-A and Ang-2. Of note, PlGF has previously been suggested as a resistance mechanism to anti-angiogenic agents. Interestingly, it does not appear to be produced by the tumor, but by the host as a systemic response [27].

DCE-MRI is a well-established imaging method to assess treatment-induced changes of vascular permeability [28]. A change in Ktrans of  $\geq 40\%$  is considered clinically significant. DCE-MRI analysis in our study confirms the mechanism of action of BI 836880 in the tumor at the recommended dose, with evidence of changes in tumor vessel permeability at doses  $\geq 120$  mg q3w. Other VEGF and/or Ang-2-targeting agents have also shown reductions in Ktrans. Administration of vanucizumab, a bispecific monoclonal antibody targeting VEGF and Ang-2, resulted in sustained post-treatment reductions in DCE-MRI parameters [24]. At doses of 30 mg/kg biweekly or weekly, vanucizumab treatment was associated with a median reduction in Ktrans of 31.4% and 29.7%, respectively. AMG 386, an anti-Ang-1/Ang-2 peptibody, showed a median Ktrans reduction of 20.3% in 10 patients within the 30 mg/kg dose cohort [29].

The two-compartment PopPK model developed based on combined data from the two Phase I studies with different dosing schedules overall provided a good description of measured plasma concentrations of BI 836880. As expected, due to its binding to HSA, BI 836880 had an extended plasma half-life of about 11 days. During covariate assessment, small effects of body weight and HSA on the PK of BI 836880 were identified. Based on the limited number of analyzed patients, the precision of the body weight exponents was, however, low, and therefore these parameters were fixed according to the allometric principle. As expected from BI 836880's binding to HSA leading to its half-life extension, patients with higher HSA levels tended to show a lower central clearance. Additional data from Phase II or Phase III studies would be needed to improve the characterization of the effects of intrinsic of extrinsic factors (covariates) on the PK of BI 836880. Based on fixed PK from the PopPK model, the PD part of the PopPK/

PD model was implemented as a mass action model, in which BI 836880 in the central compartment binds free Ang-2 and sequesters it in a complex (BI:Ang-2). A major challenge in PD model development was the handling of samples with unquantifiable free Ang-2 observed particularly at the higher dose levels of BI 836880 (free Ang-2 was quantifiable in only 25% of the 771 samples across dose levels). Due to model instabilities, it was not possible to use the method referred to as M3 [23], in which the probability of a sample being BLQ is calculated and included as part of the model's objective function. In contrast to this, merging all consecutive BLQ values to one value (assigned to LLOQ/2) gave reasonable results in terms of fitting the free Ang-2 data of individual patients and reproducing the observed patterns of samples that were BLQ. Only in the higher dose groups of study 1336.6 (weekly treatment schedule), model underpredictions of the probability of free Ang-2 being BLQ seemed to be present based on VPCs. Currently it is not known whether this is a true bias due to the high proportion of BLQs or whether it is an artefact in the VPC due to the limited number of patients per dose group, where observations were available. This potential bias was not observed for study 1336.1 including the relevant 3-week treatment schedule (q3w dosing), which was used for the simulations. Based on this, a greater uncertainty might be assumed for model predictions of free Ang-2 at higher dose levels with measured free Ang-2 values close to or below the limit of detection and estimates for free Ang-2 inhibition by the model might be considered conservative (slightly higher actual Ang-2 inhibition than predicted by the model). In general, the PopPK/PD model integrating data from the two Phase I studies and characterizing the degree and duration of Ang-2 inhibition for various dose levels on average as well as on the individual level (taking into account PK and PD variability) was considered a useful tool to support the assessment of target engagement of BI 836880 at different dose levels and to guide dose selection of BI 836880.

In conclusion, our PD analysis and PopPK/PD model supported BI 836880 720 mg q3w as a biologically relevant dose providing high target engagement based on comprehensive analyses of multiple target engagement biomarkers. Our biomarker data and model results were in agreement with the preliminary efficacy results from the Phase I studies, with responses tending to be observed in the higher dose cohorts ( $\geq 720$  mg q3w) [28]. As often in Phase I dose escalation studies, the number of patients per dose level was limited in our study, reducing the confidence in the analyses. However,

by using robust assays in combination with the PopPK/PD modeling approach, we attempted to deal with this inherent uncertainty in the best possible manner, and consider this as a potentially useful approach for other Phase I dose escalation studies. A similar binding model has been established to characterize the dynamics and interactions of xentuzumab with blood biomarkers, assessing target engagement and thereby guiding dose selection in a Phase I oncology trial [30]. For other molecules, such an approach was also chosen, e.g. PRMT5 [31, 32]. In light of Project OPTIMUS, the presented comprehensive evaluation of multiple biomarkers combined with PopPK/PD modeling can therefore serve as an example of biomarker aided dose justification/optimization during early phase of drug development in oncology. Combined with other assessments (e.g. safety and efficacy) this can support the totality of evidence approach for dose optimization in oncology as recently summarized by Gao and colleagues [33].

In addition to their well-recognized roles in angiogenesis, VEGF and Ang-2 also have immunosuppressive effects in the tumor microenvironment, promoting interest in combining anti-angiogenic agents with inhibition of the programmed cell death protein 1 (PD-1) pathway. Combination of anti-VEGF and anti-PD-1 therapy has shown efficacy in several tumor types [34, 35]. BI 836880 is currently being investigated in combination with ezabenlimab (BI 754091), an anti-PD-1 antibody, in patients with advanced solid tumors (NCT03468426 and NCT03697304). Ezabenlimab is given in a q3w schedule; based on our analyses and the clinical results, BI 836880 doses of 360, 500 and 720 mg q3w, which show biological activity, were selected for investigation.

Glossary Boxes

Glossary Box 1: Assay Development

Free, total target concentration	Free target levels are defined as the fraction of total target present in the plasma sample that is unbound to drug and still able to bind to drug at assay conditions. Total target levels are the sum of free and bound target.
Precise	Here defined as $\leq 30\%$ coefficient of variation between-runs.

Parallel/Parallelism	The ability of the assay to quantify the endogenous analyte in the same manner as the recombinant (surrogate) calibration standard. Non-spiked individual matrix samples are serially diluted and measured. The measured concentration adjusted to pure matrix should be independent from the dilution factor over a range of dilutions. Parallelism is the prerequisite for a quantitative immunoassay.
Relative quantitative manner	An assay that quantifies the analyte relative to the used (surrogate) calibration standard and the specificity of the antibodies. The measured concentration can be used for quantitative data evaluation but are not the “true” absolute concentrations of the analyte that in case of proteins most often is heterogenous and without a defined molecular weight.
Isochronic approach	A long term stability investigation approach that stresses various aliquots of stability samples at different conditions for different time periods and store them thereafter at ultra cold conditions (–150 °C) together with a non-stressed reference aliquot that has not been stored at higher temperatures. At the day of measurement all aliquots are thawed and measured together in the same run. Possible relative deviations in concentration between the stressed and the reference aliquot would indicate instability of the analyte.
Intra/Inter-assay Precision	The coefficient of variation of several results of a homogenous test sample that have been measured within a run (within-run/ assay precision) or in several runs on several days (between-run/assay precision).

### Glossary Box 2: PopPK/PD Model Development

PopPK	Population Pharmacokinetics (PopPK) analysis is a well-established, quantitative method that can explain some of the variability in drug concentrations over time among individuals. This variability can be attributed to intrinsic factors, such as differences in body weight or the presence and extent of liver or renal impairment or to extrinsic factors, such as effects of food on drug absorption. Population PK analysis has the potential to integrate all relevant PK information across a range of doses and populations to identify factors that can affect a drug’s exposure.
PopPK/PD	Population Pharmacokinetics/ Pharmacodynamics (PopPK/ PD) analysis is an extension of the PopPK analysis by additionally considering the pharmacological effect of the drug (binding and blocking of Ang2, in this example) and its variability.
Non-linear mixed effects (NLME) model	Nonlinear mixed-effects models are frequently used for pharmacokinetic and or pharmacodynamic data analysis. They account for inter-subject variability in pharmacokinetic and/ or pharmacodynamic parameters by incorporating subject-specific random effects into the model. The random effects are often assumed to follow a (multivariate) normal distribution. Using NLME models, pharmacometricians have the ability to leverage data from multiple studies, dosing routes, and administration schedules.
Interindividual variability (IIV)	The interindividual variability reflects the variance of a parameter across individuals of a population.
Interoccasion variability (IOV)	The interoccasion variability (also called Intra-individual variability) reflects a transient, within-person change of a parameter estimated as variability between different occasions.
Residual variability	Residual variability is unexplained variability after controlling for other sources of variability.

Covariates	In the current manuscript, this refers to intrinsic or extrinsic factors that can impact the pharmacokinetics behavior of a drug (e.g. factors that can affect a drug's absorption, distribution or elimination into/from the human body). Examples of intrinsic factors are patient characteristics such as the presence and extent of liver or renal impairment (potentially affecting the drugs elimination). An example of an extrinsic factor is food (potentially affecting the drugs absorption). Population PK analysis has the potential to identify factors that can affect a drug's exposure.
------------	--

## Abbreviations

ABC	Ammonium bicarbonate
ACN	Acetonitrile
ALP	Alkaline phosphatase
Ang	Angiotensin
BI	Boehringer Ingelheim
BLQ	Below the limit of quantification
Ca	Carcinoma
CI	Confidence interval
CL	Clearance
CV	Coefficient of variation
DCE-MRI	Dynamic contrast-enhanced-magnetic resonance imaging
dev	Deviation
DLT	Dose-limiting toxicity
ECOG	Eastern Cooperative Oncology Group
EDTA	Ethylenediaminetetraacetic acid
eGFR	Estimated glomerular filtration rate
ELISA	Enzyme-linked immunosorbent assay
ER+	Estrogen receptor positive
F/T	Freeze/thaw
Her2-	Human epidermal growth factor receptor 2 negative
HSA	Human serum albumin
iAUC60	Initial area under the contrast agent concentration–time curve at 60 s
IIV	Interindividual variability
IOV	Interoccasion variability
Ktrans	The volume transfer constant
LC-HRMS	Liquid chromatography high-resolution mass spectrometry
LLOQ	Lower limit of quantification
MAP	Multi-analyte profiling
MS	Mass spectrometry
MSD	Meso Scale Discovery
N/A	Not applicable
PBS	Phosphate buffered saline
PD	Pharmacodynamic
PD-1	Programmed cell death protein 1
PK	Pharmacokinetic
PIGF	Placenta growth factor
Pop	Population
Q3W	Every 3 weeks
QC	Quality control
QW	Once weekly
RBM	Rules-Based Medicine
RRID	Research Resource Identification Portal
RT	Room temperature

SISCAPA	Stable Isotope Standards and Capture by Anti-Peptide Antibodies
S/N	Signal to noise ratio
sTie2	Soluble Tie2
sVEGFR3	Soluble vascular endothelial growth factor receptor 3
TBS	Tris buffered saline
TFA	Trifluoroacetic acid
VEGF	Vascular endothelial growth factor
VPC	Visual predictive check

## Supplementary Information

The online version contains supplementary material available at <https://doi.org/10.1186/s12967-024-05612-x>.

Supplementary Material 1.

## Acknowledgements

Ralph Graeser: Boehringer Ingelheim Pharmaceuticals, Inc., Ridgefield, CT, USA: At the time of manuscript development. MRI examination and analysis were coordinated by the core facility Magnetic Resonance Development and Application Center Freiburg (MRDAC), Department of Radiology—University Medical Center Freiburg, Faculty of Medicine, University of Freiburg, registered at the Research Resource Identification Portal (RRID) under RRID:SCR\_021926.

## Author contributions

G Jayadeva, HG. Niessen, Z Oum'Hamed, and R Graeser made substantial contributions to the conception or design of the work. S Keller, U Kunz, U Schmid, J Beusmans, M Büchert, M He, G Jayadeva, D Luedtke, HG. Niessen, S Pleiner, X Wang and R Graeser made substantial contributions to the acquisition, analysis, or interpretation of data for the work. J Beusmans made substantial contributions to the creation of new software used in the work. C Le Tourneau and S Pleiner drafted the work or substantively revised it. All authors approved the final version to be published and agree to be accountable for all aspects of the work in ensuring that questions related to the accuracy or integrity of any part of the work are appropriately investigated and resolved.

## Funding

This work was supported by Boehringer Ingelheim International GmbH. Medical writing support for the development of this manuscript, under the direction of the authors, was provided by Hannah Simmons, MSc, of Ashfield MedComms, an Inizio Company and funded by Boehringer Ingelheim. The authors received no direct payment for development of the manuscript.

## Availability of data and materials

To ensure independent interpretation of clinical study results and enable authors to fulfill their role and obligations under the ICMJE criteria, Boehringer Ingelheim grants all external authors access to clinical study data pertinent to the development of the publication. In adherence with the Boehringer Ingelheim Policy on Transparency and Publication of Clinical Study Data, scientific and medical researchers can request access to clinical study data when it becomes available on Vivli—Center for Global Clinical Research Data, and earliest after publication of the primary manuscript in a peer-reviewed journal, regulatory activities are complete, and other criteria are met. Please visit [Medical & Clinical Trials|Clinical Research|MyStudyWindow](#) for further information.

## Declarations

### Ethics approval and consent to participate

The studies were conducted in accordance with the Declaration of Helsinki and Good Clinical Practice guidelines as defined by the International Conference on Harmonization; all patients provided written informed consent for study participation; and the institutional review board approved the study.

**Consent for publication**

All the authors have consented for publication.

**Competing interests**

S Keller, U Kunz, U Schmid, M He, G Jayadeva, D Luedtke, HG. Niessen, Z Oum'Hamed, S Pleiner and R Graeser are or have all been employees of Boehringer Ingelheim. J Beusmans and X Wang are employees of Metrum Research Group. M Büchert and C Le Tourneau declare no competing interests.

**Author details**

<sup>1</sup>Boehringer Ingelheim Pharma GmbH & Co. KG, Biberach, Germany. <sup>2</sup>Metrum Research Group, Tariffville, CT, USA. <sup>3</sup>Medical Center University of Freiburg, Faculty of Medicine, University of Freiburg, Freiburg, Germany. <sup>4</sup>Boehringer Ingelheim Pharmaceuticals, Inc., Ridgefield, CT, USA. <sup>5</sup>Boehringer Ingelheim International GmbH, Ingelheim am Rhein, Germany. <sup>6</sup>Department of Drug Development and Innovation (D3i), Institut Curie, INSERM U900 Research Unit, Paris-Saclay University, Saint-Cloud, Paris, France. <sup>7</sup>Pieris Pharmaceuticals GmbH, Zeppelinstrasse 3, 85399 Hallbergmoos, Germany.

Received: 21 March 2024 Accepted: 18 August 2024

Published online: 14 October 2024

**References**

- World Health Organization. Global cancer burden growing, amidst mounting need for services. <https://www.who.int/news/item/01-02-2024-global-cancer-burden-growing-amidst-mounting-need-for-services>. Accessed 07 Aug 2024.
- Bray F, Laversanne M, Sung H, Ferlay J, Siegel RL, Soerjomataram I, Jemal A. Global cancer statistics 2022: GLOBOCAN estimates of incidence and mortality worldwide for 36 cancers in 185 countries. *CA Cancer J Clin*. 2024;74:229–63. <https://doi.org/10.3322/caac.21834>.
- Anand U, Dey A, Chandel AKS, Sanyal R, Mishra A, Pandey DK, De Falco V, Upadhyay A, Kandimalla R, Chaudhary A, Dhanjal JK, Dewanjee S, Vallamkondur J, de la Lastra JMP. Cancer chemotherapy and beyond: current status, drug candidates, associated risks and progress in targeted therapeutics. *Genes Dis*. 2023;10:1367–401. <https://doi.org/10.1016/j.gendis.2022.02.007>.
- Akbarali HI, Muchhala KH, Jessup DK, Cheatham S. Chemotherapy induced gastrointestinal toxicities. *Adv Cancer Res*. 2022;155:131–66. <https://doi.org/10.1016/bs.acr.2022.02.007>.
- Hanahan D, Weinberg RA. Hallmarks of cancer: the next generation. *Cell*. 2011;144:646–74. <https://doi.org/10.1016/j.cell.2011.02.013>.
- Close A. Antiangiogenesis and vascular disrupting agents in cancer: circumventing resistance and augmenting their therapeutic utility. *Fut Med Chem*. 2016;8:443–62. <https://doi.org/10.4155/fmc.16.6>.
- Ferrara N, Adams AP. Ten years of anti-vascular endothelial growth factor therapy. *Nat Rev Drug Discov*. 2016;15:385–403. <https://doi.org/10.1038/nrd.2015.17>.
- Kerbel RS. Tumor angiogenesis. *New Eng J Med*. 2008;358:2039–49. <https://doi.org/10.1056/NEJMra0706596>.
- García J, Hurwitz HI, Sandler AB, Miles D, Coleman RL, Deurloo R, Chinot OL. Bevacizumab (Avastin®) in cancer treatment: a review of 15 years of clinical experience and future outlook. *Cancer Treat Rev*. 2020;86:102017. <https://doi.org/10.1016/j.ctrv.2020.102017>.
- Lambrechts D, Lenz HJ, de Haas S, Carmeliet P, Scherer SJ. Markers of response for the antiangiogenic agent bevacizumab. *J Clin Oncol*. 2013;31:1219–30. <https://doi.org/10.1200/jco.2012.46.2762>.
- Thurston G, Daly C. The complex role of angiopoietin-2 in the angiopoietin-tie signaling pathway. *Cold Spring Harb Persp Med*. 2012;2:a006550. <https://doi.org/10.1101/cshperspect.a006550>.
- Hashizume H, Falcón BL, Kuroda T, Baluk P, Coxon A, Yu D, Bready JV, Oliner JD, McDonald DM. Complementary actions of inhibitors of angiopoietin-2 and VEGF on tumor angiogenesis and growth. *Cancer Res*. 2010;70:2213–23. <https://doi.org/10.1158/0008-5472.Can-09-1977>.
- Brown JL, Cao ZA, Pinzon-Ortiz M, Kendrew J, Reimer C, Wen S, Zhou JQ, Tabrizi M, Emery S, McDermott B, Pablo L, McCoon P, Bedian V, Blakey DC. A human monoclonal anti-ANG2 antibody leads to broad antitumor activity in combination with VEGF inhibitors and chemotherapy agents in preclinical models. *Mol Cancer Ther*. 2010;9:145–56. <https://doi.org/10.1158/1535-7163.Mct-09-0554>.
- Hofmann I, Baum A, Hilberg F, Garin Chesa P, Depla E, Boucneau J, Kraut N, Künkele K-P. Dual targeting of angiogenesis pathways: combined blockade of VEGF and Ang2 signaling. Data presented at the 8th Euro Global Summit on Cancer Therapy. November 3–5, 2015; Valencia, Spain. 2015.
- Le Tourneau C, Becker H, Claus R, Elez E, Ricci F, Fritsch R, Silber Y, Hennequin A, Tabernero J, Jayadeva G, Luedtke D, He M, Isambert N. Two phase I studies of BI 836880, a vascular endothelial growth factor/angiopoietin-2 inhibitor, administered once every 3 weeks or once weekly in patients with advanced solid tumors. *ESMO Open*. 2022;7:100576. <https://doi.org/10.1016/j.esmoop.2022.100576>.
- Moon H. FDA initiatives to support dose optimization in oncology drug development: the less may be the better. *Transl Clin Pharmacol*. 2022;30:71–4. <https://doi.org/10.12793/tcp.2022.30.e9>.
- Qi T, Dunlap T, Cao Y. Embracing project optimus: can we leverage evolutionary theory to optimize dosing in oncology? *Pharm Res*. 2022;39:3259–65. <https://doi.org/10.1007/s11095-022-03380-1>.
- Shah M, Rahman A, Theoret MR, Pazdur R. The drug-dosing conundrum in oncology—when less is more. *N Engl J Med*. 2021;385:1445–7. <https://doi.org/10.1056/NEJMp2109826>.
- Venkatakrishnan K, van der Graaf PH. Toward project optimus for oncology precision medicine: multi-dimensional dose optimization enabled by quantitative clinical pharmacology. *Clin Pharmacol Ther*. 2022;112:927–32. <https://doi.org/10.1002/cpt.2742>.
- Tofts PS. Modeling tracer kinetics in dynamic Gd-DTPA MR imaging. *J Magn Res Imag*. 1997;7:91–101. <https://doi.org/10.1002/jmri.1880070113>.
- Kunz U, Goodman J, Loevgren U, Piironen T, Elsy K, Robinson P, Pihl S, Versteilen A, Companjen A, Fjording MS, Timmerman P. Addressing the challenges of biomarker calibration standards in ligand-binding assays: a European Bioanalysis Forum perspective. *Bioanal*. 2017;9:1493–508. <https://doi.org/10.4155/bio-2017-0141>.
- Banks RE, Forbes MA, Kinsey SE, Stanley A, Ingham E, Walters C, Selby PJ. Release of the angiogenic cytokine vascular endothelial growth factor (VEGF) from platelets: significance for VEGF measurements and cancer biology. *Br J Cancer*. 1998;77:956–64. <https://doi.org/10.1038/bjc.1998.158>.
- Beal SL. Ways to fit a PK model with some data below the quantification limit. *J Pharmacokinetic Pharmacodyn*. 2001;28:481–504. <https://doi.org/10.1023/a:1012299115260>.
- Hidalgo M, Martínez-García M, Le Tourneau C, Massard C, Garralda E, Boni V, Taus A, Albanell J, Sablin MP, Alt M, Bahleda R, Varga A, Boetsch C, Franjkovic I, Heil F, Lahr A, Lechner K, Morel A, Nayak T, Rossomanno S, Smart K, Stubenrauch K, Krieter O. First-in-human phase I study of single-agent vanucizumab, a first-in-class bispecific anti-angiopoietin-2/anti-VEGF-A antibody, in adult patients with advanced solid tumors. *Clin Canc Res*. 2018;24:1536–45. <https://doi.org/10.1158/1078-0432.Ccr-17-1588>.
- Azzariti A, Porcelli L, Brunetti O, Del Re M, Longo V, Nardulli P, Signorile M, Xu JM, Calabrese A, Quatrone AE, Miallo E, Lorusso V, Silvestris N. Total and not bevacizumab-bound vascular endothelial growth factor as potential predictive factors to bevacizumab-based chemotherapy in colorectal cancer. *World J Gastroenterol*. 2016;22:6287–95. <https://doi.org/10.3748/wjg.v22.i27.6287>.
- Loupakis F, Falcone A, Masi G, Fioravanti A, Kerbel RS, Del Tacca M, Bocci G. Vascular endothelial growth factor levels in immunodepleted plasma of cancer patients as a possible pharmacodynamic marker for bevacizumab activity. *J Clin Oncol*. 2007;25:1816–8. <https://doi.org/10.1200/jco.2006.10.3051>.
- Bagley RG, Ren Y, Weber W, Yao M, Kurtzberg L, Pinckney J, Bangari D, Nguyen C, Brondyk W, Kaplan J, Teicher BA. Placental growth factor upregulation is a host response to antiangiogenic therapy. *Clin Canc Res*. 2011;17:976–88. <https://doi.org/10.1158/1078-0432.Ccr-10-2687>.
- O'Connor JP, Jackson A, Parker GJ, Jayson GC. DCE-MRI biomarkers in the clinical evaluation of antiangiogenic and vascular disrupting agents. *Brit J Canc*. 2007;96:189–95. <https://doi.org/10.1038/sj.bjc.6603515>.
- Herbst RS, Hong D, Chap L, Kurzrock R, Jackson E, Silverman JM, Rasmussen E, Sun YN, Zhong D, Hwang YC, Evelhoch JL, Oliner JD, Le N, Rosen LS. Safety, pharmacokinetics, and antitumor activity of AMG 386, a selective angiopoietin inhibitor, in adult patients with advanced solid tumors. *J Clin Oncol*. 2009;27:3557–65. <https://doi.org/10.1200/jco.2008.19.6683>.

30. Parra-Guillen ZP, Schmid U, Janda A, Freiwald M, Troconiz IF. Model-informed dose selection for xentuzumab, a dual insulin-like growth factor- $\alpha$ / $\beta$ -neutralizing antibody. *Clin Pharmacol Ther*. 2020;107:597–606. <https://doi.org/10.1002/cpt.1648>.
31. Guo C, Liao KH, Li M, Wang IM, Shaik N, Yin D. PK/PD model-informed dose selection for oncology phase I expansion: case study based on PF-06939999, a PRMT5 inhibitor. *CPT Pharmacomet Syst Pharmacol*. 2023;12:1619–25. <https://doi.org/10.1002/psp4.12882>.
32. Garralda E, Dienstmann R, Tabernero J. Pharmacokinetic/pharmacodynamic modeling for drug development in oncology. *Am Soc Clin Oncol Educ Book*. 2017;37:210–5. [https://doi.org/10.1200/EDBK\\_180460](https://doi.org/10.1200/EDBK_180460).
33. Gao W, Liu J, Shtylla B, Venkatakrishnan K, Yin D, Shah M, Nicholas T, Cao Y. Realizing the promise of project optimus: challenges and emerging opportunities for dose optimization in oncology drug development. *CPT Pharmacomet Syst Pharmacol*. 2024;13:691–709. <https://doi.org/10.1002/psp4.13079>.
34. Finn RS, Qin S, Ikeda M, Galle PR, Ducreux M, Kim TY, Kudo M, Breder V, Merle P, Kaseb AO, Li D, Verret W, Xu DZ, Hernandez S, Liu J, Huang C, Mulla S, Wang Y, Lim HY, Zhu AX, Cheng AL. Atezolizumab plus bevacizumab in unresectable hepatocellular carcinoma. *New Engl J Med*. 2020;382:1894–905. <https://doi.org/10.1056/NEJMoa1915745>.
35. Socinski MA, Jotte RM, Cappuzzo F, Orlandi F, Stroyakovskiy D, Nogami N, Rodríguez-Abreu D, Moro-Sibilot D, Thomas CA, Barlesi F, Finley G, Kelsch C, Lee A, Coleman S, Deng Y, Shen Y, Kowanetz M, Lopez-Chavez A, Sandler A, Reck M. Atezolizumab for first-line treatment of metastatic nonsquamous NSCLC. *New Engl J Med*. 2018;378:2288–301. <https://doi.org/10.1056/NEJMoa1716948>.

## Publisher's Note

Springer Nature remains neutral with regard to jurisdictional claims in published maps and institutional affiliations.